

Lawrence Berkeley National Laboratory

Recent Work

Title

HIGH ENERGY NUCLEUS-NUCLEUS COLLISIONS AT CERN: SIGNATURE, PHYSICAL OBSERVABLES AND EXPERIMENTAL RESULTS

Permalink

<https://escholarship.org/uc/item/9fq4d7mb>

Author

Harris, J.W.

Publication Date

1988-02-01

c.2



Lawrence Berkeley Laboratory

UNIVERSITY OF CALIFORNIA

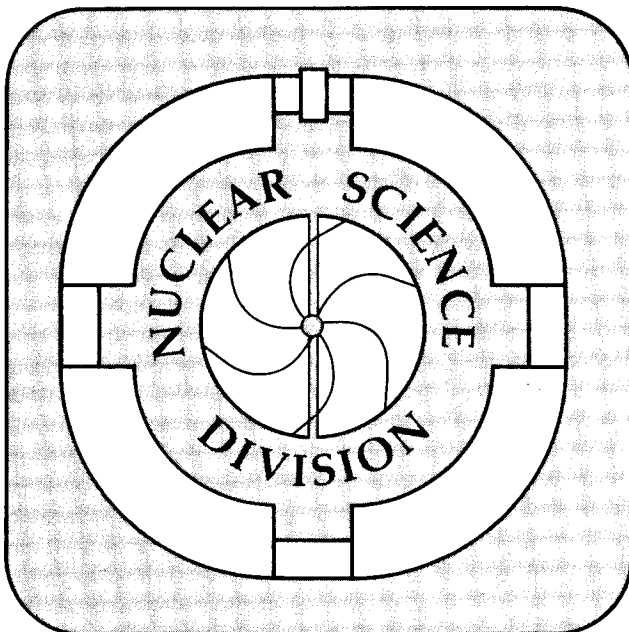
Presented at the XI Symposium on Nuclear Physics,
Oaxtepec, Mexico, January 4-7, 1988

LIBRARY AND DOCUMENTS SECTION
SEP 03 1988

High Energy Nucleus-Nucleus Collisions at CERN: Signature, Physical Observables and Experimental Results

J.W. Harris

February 1988



LBL-24772
c.2

DISCLAIMER

This document was prepared as an account of work sponsored by the United States Government. While this document is believed to contain correct information, neither the United States Government nor any agency thereof, nor the Regents of the University of California, nor any of their employees, makes any warranty, express or implied, or assumes any legal responsibility for the accuracy, completeness, or usefulness of any information, apparatus, product, or process disclosed, or represents that its use would not infringe privately owned rights. Reference herein to any specific commercial product, process, or service by its trade name, trademark, manufacturer, or otherwise, does not necessarily constitute or imply its endorsement, recommendation, or favoring by the United States Government or any agency thereof, or the Regents of the University of California. The views and opinions of authors expressed herein do not necessarily state or reflect those of the United States Government or any agency thereof or the Regents of the University of California.

High Energy Nucleus-Nucleus Collisions at CERN: Signatures, Physical Observables and Experimental Results

John W. Harris

Nuclear Science Division, Lawrence Berkeley Laboratory,
University of California, Berkeley, CA 94720, USA

Abstract

Experimental results on high energy nucleus-nucleus collisions have become available with the recent experiments at CERN utilising 200 GeV/n oxygen and sulphur beams. Physics motivations for these experiments are presented: a description of predicted signatures for possible formation of a quark-gluon plasma and physical observables that are expected to provide important information for understanding the dynamics of these collisions. A presentation will be made of some of the first experimental results to emerge from this new field.

1. Introduction

The formation of a quark-gluon plasma in very high energy collisions of heavy nuclei has been predicted in various theoretical approaches. In the collision process energy and baryon densities increase and are expected to reach critical values where the quark constituents of the incident nucleons, bound in nuclei, form an extended volume of freely interacting quarks, antiquarks and gluons. Simple estimates of these critical values for formation can be made. For example, the critical baryon density $\rho_B^{critical}$ for deconfinement to occur may be approximated by the density at which the nucleons are tightly-packed, completely filling the nuclear volume. With ρ_0 the density of normal nuclear matter, the ratio $\rho_B^{critical}/\rho_0 \approx (\text{volume of normal nucleus } A)/(\text{volume of } A \text{ nucleon bags tightly-packed together}) \approx (1.25 \times A^{1/3})^3 / (A \times (0.75)^3)$. This gives $\rho_B^{critical} \approx 5\rho_0$. An estimate of the critical energy density would be the energy of A nucleons compressed into the volume of A nucleon bags tightly-packed together: $\epsilon^{critical} \approx (A \times \text{nucleon mass})/(A \times (0.75)^3) \approx 2\text{-}3 \text{ GeV}/\text{fm}^3$. This should be compared to the energy densities of a hadron $\epsilon_{hadron} \approx 0.5 \text{ GeV}/\text{fm}^3$ and of a nucleus $\epsilon_{nucleus} \approx 0.15 \text{ GeV}/\text{fm}^3$. The system must sustain these conditions for a time longer than the transition time of the two interacting nuclei in order for the quark-gluon plasma phase to form without dilution by subsequent interactions. These high baryon

and energy densities necessary for the formation of a quark-gluon plasma may best be reached in collisions of heavy nuclei at very high energies given adequate thermalisation.

Recent lattice quantum chromodynamics calculations^{1,2} predict a phase transition from a hadronic gas to a quark-gluon plasma. The critical values predicted² by these calculations are $\epsilon^{critical} \approx 2 \text{ GeV}/\text{fm}^3$, at a critical temperature $T^{critical} \approx 200\text{-}250 \text{ MeV}$. The relationship of this phase transition to the various phases of nuclear matter can be seen in Fig.1. Presented is a phase diagram for nuclear matter. In most scenarios of cosmology, a quark-gluon plasma should have existed less than a second after the Big Bang. In astrophysics, the plasma may exist in the cores of neutron stars and in other dense stellar objects. Very high energy nucleus-nucleus collisions may provide the conditions necessary for formation of a quark-gluon plasma and a means of studying it in the laboratory.

While possible formation of a quark-gluon plasma is the underlying motivation for this field of physics, a study of the dynamics of the collision processes is of fundamental importance to understanding the microscopic structure of hadronic interactions at high densities, at the level of quarks and gluons, and the conditions for formation of the plasma. The predicted signatures of quark-gluon plasma formation will be described in section 2. Physical observables necessary for understanding the dynamics of the collisions, a precursor to confirming plasma formation, will be described in section 3. An overview of the experiments and some of the important physics results to date addressing plasma signatures and physical observables will be presented in section 4. A brief summary and conclusions will be made in section 5.

2. Possible Signatures of Quark-Gluon Plasma Formation

2.1 Strange Particle Production

One of the earliest predictions for a signature of the deconfinement transition is an enhancement of s and \bar{s} quarks in a quark-gluon plasma in thermal and chemical equilibrium.³ The strangeness enhancement is a result of the Pauli principle suppression of $u\bar{u}$ and $d\bar{d}$ pair production in favor of $s\bar{s}$ pairs in the initial u and d -rich environment remaining from the incident nuclei. Furthermore, the \bar{u} and \bar{d} quarks annihilate with u and d quarks, while the $\bar{s}s$ annihilation occurs less frequently until saturation of the s and \bar{s} abundances. Most calculations predict an enhancement in the observed \bar{s} yield

as a signature of plasma formation while s quark yields, although enhanced, differ only slightly in a plasma compared to a hadron gas. It has recently been noted⁴ that the actual observation of \bar{s} enhancement after plasma formation is severely complicated by the spacetime evolution of the collision process, making it difficult to discriminate between the hadronisation products of a quark-gluon plasma and those of a chemically-equilibrated hadron gas. However, it is highly unlikely that hadronic processes in the nonplasma phase are best represented by an equilibrium hadron gas. In any case the dynamics complicate the issue and must be understood.

Dynamical approaches have recently predicted^{5,6} a separation of strangeness during the hadronisation process. During the mixed phase, consisting of plasma and hadron gas and following the plasma phase, the hadron gas becomes \bar{s} -rich due to radiation-cooling from K^+ and K^0 emission. This leaves behind an s-enriched plasma and may manifest itself in the slopes of the observed K^+ and K^- spectra⁷ as well as the possible production of strange droplets of matter.⁸

2.2 J/ψ Suppression

In analogy to the Debye screening of electrons in electrodynamics and plasma physics, Debye screening of the quark color charge results in deconfinement into a quark-gluon plasma. Furthermore, the color screening is predicted⁹ to prevent $c\bar{c}$ binding into a J/ψ in the deconfinement region. In hadron-hadron collisions $c\bar{c}$ pairs can be produced in either gg or $q\bar{q}$ interactions. However, in nucleus-nucleus collisions the $c\bar{c}$ will appear in a deconfining environment at high temperature and density. Therefore, if the Debye radius is less than the radius of the J/ψ at temperature T , then formation of the J/ψ is prohibited assuming the plasma lifetime is longer than the formation time of the J/ψ from $c\bar{c}$. Thus observation of J/ψ suppression in nucleus-nucleus interactions might signify formation of the plasma. This is a possible signature since the J/ψ yield would not be reduced in passage through the nuclear matter due to its small nuclear absorption.¹⁰

A recent calculation¹¹ suggests that it may be possible to capture the $c\bar{c}$ in a resonant state which adiabatically evolves into a bound state of J/ψ after the temperature decreases. A consideration of the timescales for formation of the $c\bar{c}$ pair into a Bohr-Debye bound state yields values of the formation time $6 \leq \tau_f(c\bar{c}) \leq 43$ fm/c which may be of the order of the lifetime of the quark-gluon plasma. This could sig-

nificantly diminish the expected J/ψ suppression by the plasma.

2.3 Mean Transverse Momentum and Temperature

In analogy to the phase change of melting ice, that of the deconfinement transition from hadrons to quark-gluon plasma can be represented by the diagram in Fig.2. The temperature of the system increases as the energy is increased until the transition temperature. At this point the phase transition occurs and the temperature remains constant with the two phases coexisting until all matter has undergone the transition. Above this point the temperature will then increase again as the energy increases. If it were possible to measure the temperature of the system as a function of incident energy, a signature of the phase transition would be an observation of the behavior exhibited in Fig.2. Measuring the mean transverse momentum $\langle p_{\perp} \rangle$ of hadrons, which reflects the temperature,¹² has been proposed.¹³ However, a complication of this scheme is that the temperatures reflected in most p_{\perp} spectra correspond to the freezeout stage of the expansion after cooling. It has therefore been proposed that direct photons or dilepton pairs be measured since their interaction probabilities with nuclear matter are small. These probes should then provide information on the hot plasma phase of the collision process.

Correlations between $\langle p_{\perp} \rangle$ and the multiplicity per unit rapidity dN/dy are predicted¹⁴ to reflect a phase transition in the collision process. The lower multiplicities per unit rapidity would reflect the temperature of the hadronic matter and the higher multiplicities that of the plasma phase. The predicted correlation shown in Fig.3 should be similar to Fig.2 with energy replaced by dN/dy . Since the number of particles produced per unit rapidity dN/dy reflects the energy available for particle production, it can be used as a measure of the energy necessary to heat the system. Since the temperature and the phase of the system change as a function of time in any given nucleus-nucleus collision, the prediction of Fig.3 can be generated from a set of data collected at one incident energy.

2.4 Fluctuations of Transverse Energy and Multiplicity

Event-by-event fluctuations of the transverse energy per unit rapidity have been proposed¹⁵ as a signature of a first-order phase transition. With such a transition large amounts of

energy will be liberated in the system, perhaps localised in space, leading to deflagration or detonation and explosion. These localised explosions result in large fluctuations in the production of matter and energy as a function of the rapidity of the products. Therefore, distributions of dE_{\perp}/dy or dN/dy as a function of rapidity y may exhibit large fluctuations at the rapidities of the deflagrations or detonations providing possible signatures of plasma formation.

3. Physical Observables of the Reaction Dynamics

In addition to the importance of the physical observables described in the previous section as possible signatures of quark-gluon plasma formation, these and other observables provide information on the dynamics of very high energy and high density nuclear interactions. *Multiplicity distributions* per unit rapidity dN_i/dy for individual particle types (i) as a function of rapidity may provide an indication of the particle densities reached in the collisions. The multiplicity distributions by comparison with geometrical models and distributions from hadron-hadron collisions can be used to determine the geometry of the nucleus-nucleus collisions. *Transverse energy E_{\perp} distributions* reflect the degree to which the incident energy of the nuclei thermalises in the collision process, i.e. the "stopping power". The E_{\perp} distribution can also be used to estimate the energy density reached in the collisions. *Particle abundances and spectra* are important to determining the s and \bar{s} content, baryon number content and mean transverse momenta (temperatures) of the various constituents of the collisions. This information as a function of rapidity would provide a wealth of information on the dynamics of the collision process. *Hanbury Brown and Twiss correlations* between identical pions or kaons may provide information on the spacetime geometry of the system as well as information on the hadronisation process complementary to that obtained in hadron-hadron and e^+e^- interactions. It is particularly important to cross-correlate as many physical observables as possible in a given set of data, compare results with those of hadron-hadron(hh) and hadron-nucleus (hA) interactions, and to compare with results of dynamical models describing hh and hA collisions which extrapolate to the nucleus-nucleus case via geometry.

4. Experimental Results

The first laboratory experiments aimed at searching for possible plasma signatures and studying physical observables in very high energy nucleus-nucleus collisions have recently been completed at CERN. These experiments used 60 and 200 GeV/nucleon ^{16}O and ^{32}S beams to bombard a wide mass range of targets. A typical central collision event as viewed in the streamer chamber of the NA35 Collaboration¹⁶ is presented in Fig.4. The events are very complex with a large multiplicity of charged-particles. To the right of Fig.4 is drawn the typical acceptance, for 200 GeV/nucleon incident energy, of downstream calorimeters employed by most experiments to measure the energy flux of the events. A "projectile fragmentation calorimeter" covering polar angles $0^\circ \leq \theta_{lab}^{proj.frag.} \leq 0.3^\circ$ relative to the beam direction measures the energy flux remaining in the projectile fragmentation region. A "midrapidity calorimeter" measures the energy flux of particles produced at midrapidity where $2.5^\circ \leq \theta_{lab}^{midrapidity} \leq 12.5^\circ$. The correlation between these two energy fluxes is displayed in Fig.5 as observed by the WA80 Collaboration.¹⁷ These calorimeter measurements serve to classify the events by centrality. Central collisions, i.e. small impact parameter interactions, are distinguished by a small energy flux in the projectile fragmentation region and a large energy flux in the midrapidity region. Each experiment consists of this complement of calorimetry and thus is capable of triggering on the violent central collisions, where conditions for formation of the quark-gluon plasma may best be met. Other detectors, specific to each individual experiment, are then used to study plasma signatures and physical observables in these collisions.

4.1 Results on Signatures

Results on the *production of strange particles* are very preliminary at this stage of the analysis. The NA35 Collaboration has reported¹⁸ Λ , $\bar{\Lambda}$ and K^0 ratios for $^{16}\text{O} + \text{Au}$ and $p + \text{Au}$ reactions. Improved experimental efficiency calculations are necessary before reliable comparisons with theory can be made. Analysis of strange particle yields from the high statistics spectrometer experiment of the WA85 Collaboration¹⁹ and the time projection chamber of the NA36 Collaboration²⁰ are in progress. It is still too early for experimental results which may address the question of the separation of strangeness between the plasma and hadronic phases.

The NA38 Collaboration²¹ has reported preliminary finding of J/ψ suppression in

high transverse energy (E_{\perp}) events. Using a muon pair spectrometer with associated calorimetry the group observes a reduction in the J/ψ peak-to-background ratio of approximately 30 percent for high E_{\perp} events. This is observed in 200 GeV/nucleon $^{16}\text{O} + \text{U}$ collisions but not for $\text{p} + \text{U}$ collisions. In addition, the suppression is reported to occur for low transverse momentum pairs of $\mu^+\mu^-$ as predicted for plasma formation. These results are presently undergoing further scrutiny by the NA38 group, namely an attempt to understand the behavior of the background of $\mu^+\mu^-$ pairs for low and high E_{\perp} events.

The *mean transverse momentum* $\langle p_{\perp} \rangle$ has been measured for direct photons by the WA80 Collaboration.²² Displayed in Fig.6 is $\langle p_{\perp} \rangle$ as a function of $dN/d\eta$, where η is the pseudorapidity. These results look surprisingly similar to the predictions for a phase transition seen in Fig.3. *Fluctuations in transverse energy and multiplicity* as a function of rapidity have not been statistically significant in the CERN experimental results thus far.

4.2 Results on Reaction Dynamics

A study²³ of the cross sections and *multiplicity distributions* of charged particles for 60 and 200 GeV/nucleon ^{16}O projectiles by the NA35 collaboration has shown that the interaction cross sections follow a geometrical dependence on the nuclear radii and the multiplicity distributions are approximately consistent with a convolution of nucleon-nucleus collisions. It will be interesting to see if this is also true for heavier projectiles, since ^{16}O is rather light and its nucleons lie predominantly on the surface.

Experimental results on the *transverse energy distributions* have appeared from most of the CERN collaborations and are quite consistent. Displayed in Fig.7 are the E_{\perp} distributions for 60 and 200 GeV/nucleon ^{16}O on Al, Ag and W from the NA34 Collaboration²⁴ for the range $-0.1 < \eta_{lab} < 2.9$. The E_{\perp} is observed to increase with the incident energy and the target mass. The curves correspond to fits to a geometrical overlap integral with the smaller impact parameters contributing to successively higher E_{\perp} 's. These conclusions are consistent with those of Ref.16 where E_{\perp} distributions for an almost complimentary pseudorapidity range, $2.2 < \eta_{lab} < 3.8$, have similar shapes but slightly lower values of E_{\perp} . Taking the two sets of E_{\perp} distributions together an estimate of the $\langle E_{\perp} \rangle$ for 200 GeV/n $^{16}\text{O} + \text{W}$ (or Pb) central collisions is $\langle E_{\perp} \rangle \approx 200$ GeV. This corresponds to approximately 55 percent

of the total c.m. energy in the collision, assuming equipartition of the incident energy among the available degrees of freedom, and is suggestive of a fairly large degree of nuclear stopping in these collisions. The WA80 Collaboration has translated its E_{\perp} distributions into energy densities¹⁷ using the Bjorken formula.²⁵ The results shown in Fig.8 suggest fairly large energy densities are reached with values near those necessary for plasma formation.

Many of the results on *particle abundances and spectra* are still premature due to the tremendous difficulty in tracking and particle identification at such high multiplicities and energies. Results from the NA34, NA35 and WA80 Collaborations show that the pion spectra in 200 GeV/n ^{16}O interactions on various targets are similar to those from proton-nucleus collisions at the same incident energy. This is not too surprising since the pion spectra basically reflect conditions after hadronisation and freezeout. One interesting result²⁶ is that the transverse momentum distributions exhibit an excess of particles with $p_{\perp} < 0.2$ GeV/c and $p_{\perp} > 1.0$ GeV/c as in high multiplicity hadron-hadron collisions. Explanations for these results must be found at the quark level.

Hanbury Brown and Twiss correlations between negative pions have been measured by the NA35 Collaboration. A summary of the results of part of the analysis²⁷ is displayed in Fig.9. This approach involves a Gaussian parameterisation of the pion-emitting source where R_T is the transverse radius, R_L the longitudinal radius and Λ the chaoticity parameter. When $\Lambda = 1$ the source is totally chaotic. Values of $\Lambda < 1$ correspond to decreasing chaoticity, with $\Lambda = 0$ total coherence.²⁸ Pions near midrapidity in the effective $^{16}\text{O} + \text{Au}$ center-of-mass originate from a large ($R_T \approx 8$ fm), almost spherical and chaotic source. Pions over the large rapidity range reflect a much smaller source ($R_T \approx 4$ fm), with much less chaoticity. This picture suggests the formation of a thermalised fireball at midrapidity. Away from midrapidity the transverse size is near that of the incident projectile, the longitudinal size is small reflecting a correlation length of $\Delta y \approx 1$, and the chaoticity parameter is low, near that of e^+e^- and hadron-hadron collisions. The spacetime evolution of these collisions is of course much more complicated with possible phase changes and subsequent hadronisation and will be the source of much interest and debate for some time to come.

5. Summary and Conclusions

At this early stage in the study of very high energy nucleus-nucleus reactions, both the theory and experiment have provided us with some very exciting results. The predicted signatures of quark-gluon plasma formation still require much work on the part of experimentalists to be able to make reliable quantitative statements about the existence of plasma formation and on the part of theoreticians to refine predictions using the understanding of the dynamics that is starting to develop from experiments. The possibilities to use heavier projectiles up to Pb in the near future and higher energies in a collider in the foreseeable future make this a very exciting and promising young field.

Acknowledgements

The author would like to thank R. Stock and M. Gyulassy for many enlightening discussions on this subject, H. Pugh for helpful comments, fellow members of the NA35 Collaboration for encouragement and the Alexander von Humboldt Foundation of West Germany for its support during part of this work. This work was supported by the Director, Office of Energy Research, Division of Nuclear Physics of the Office of High Energy and Nuclear Physics of the U.S. Department of Energy under contract DE-AC03-76SF00098.

References

1. J. Cleymans, R.V. Gavai and E. Suhonen, Phys. Rep. 130 (1986) 217; and see Quark Matter '86, Proceedings of the Fifth International Conference on Ultra-Relativistic Nucleus-Nucleus Collisions, Asilomar, California, April 13-17, 1986 published in Nuc. Phys. A461 (1987).
2. J. Kogut, H. Matsuoka, M. Stone, H.W. Wyld, S. Shenker, J. Shigemitsu and D.K. Sinclair, Phys. Rev. Lett. 51 (1983) 869.
3. R. Hagedorn and J. Rafelski, Phys. Lett. 97B (1980) 180.
4. K.S. Lee, M.J. Rhoades-Brown and U. Heinz, Stony Brook Preprint (1987).
5. U. Heinz, K.S. Lee and M.J. Rhoades-Brown, Mod. Phys. Lett. A2 (1987) 153.
6. C. Greiner, P. Koch and H. Stöcker, U. Frankfurt Preprint UFTP 189 (1986).
7. U. Heinz, K.S. Lee and M.J. Rhoades-Brown, Phys. Rev. Lett. 58 (1987) 2292.

8. E. Witten, Phys. Rev. D30 (1984) 272.
9. T. Matsui and H. Satz, Phys. Lett. B178 (1986) 416.
10. U. Camerini et al., Phys. Rev. 35 (1975) 483.
B. Knapp et al., Phys. Rev. Lett. 34 (1975) 1040.
R. Anderson et al., Phys. Rev. Lett. 38 (1977) 263.
J. Branson et al., Phys. Rev. Lett. 38 (1977) 1334.
11. J. Kapusta, U. Minnesota Preprint, June 1987.
12. K. Redlich and H. Satz, Phys. Rev. D33 (1986) 3747.
13. E.V. Shuryak and O.V. Zhirov, Phys. Lett. B89 (1980) 253
and Phys. Lett. B171 ((1986) 99.
14. L. Van Hove, Phys. Lett. 118B (1982) 138.
15. L. Van Hove, Z. Phys. C27 (1985) 135.
16. A. Bamberger et al. (NA35 Collaboration), Phys. Lett. B184 (1987) 271.
17. R. Albrecht et al. (WA80 Collaboration), GSI Preprint GSI-87-60 (1987),
submitted to Physics Letters.
18. G. Vezstergombi et al. (NA35 Collaboration) to be published in Z. Phys. C.
19. WA85 Collaboration see Experiments at CERN in 1987, CERN Report 1987.
20. NA36 Collaboration see Experiments at CERN in 1987, CERN Report 1987.
21. NA38 Collaboration see Experiments at CERN in 1987, CERN Report 1987 and
see Quark Matter '87 to be published in Z. Phys. C.
22. R. Albrecht et al. (WA80 Collaboration), GSI Preprint GSI-87-82 (1987).
23. A. Bamberger et al. (NA35 Collaboration), submitted to Physics Letters.
24. W.J. Willis (NA34 Collaboration), preprint, IEEE Meeting, San Francisco 1987.
25. J.D. Bjorken, Phys. Rev. D27 (1983) 140.
26. H. Stroebele et al. (NA35 Collaboration), to be published in Z. Phys. C.
27. A. Bamberger et al. (NA35 Collaboration), LBL Report LBL-24646 (1987) to be published
in Physics Letters.
28. It has been suggested that values of $\Lambda < 1$ may simply reflect shortcomings in the model
being used for the source parameterisation; K. Kolehmainen and M. Gyulassy,
Phys. Lett. B180 (1986) 203 and M. Gyulassy, private communication.

Figure Captions

1. Phase diagram for nuclear matter in terms of temperature as a function of

nuclear matter density. In the lower left corner is the regime of normal nuclear matter and the right corner that of the quark-gluon plasma. Possible trajectories for cooling of the early universe, neutron star evolution and high energy heavy ion collisions are shown.

2. Temperature as a function of time, energy or heat content for the changes in phase of H₂O. The hadron gas to quark-gluon plasma phase change is analogous to either of the phase changes depicted. The vertical axis can either be the temperature or the mean transverse momentum and the horizontal axis the time or available energy.

3. Correlation of mean transverse momentum $\langle p_{\perp} \rangle$, a measure of temperature, with dn/dy as suggested by Van Hove¹⁴ indicating a phase transition.

4. NA35 Streamer Chamber event¹⁶ for 200 GeV/n ¹⁶O + Pb. To the right is a schematic diagram of the acceptances of a "projectile fragmentation calorimeter" $0^{\circ} \leq \theta_{lab}^{proj. frag.} \leq 0.3^{\circ}$ and a "midrapidity calorimeter" $2.5^{\circ} \leq \theta_{lab}^{midrapidity} \leq 12.5^{\circ}$ included in most experiments.

5. Correlation between the energy flux in the "midrapidity calorimeter" (E_T) and the "projectile fragmentation calorimeter" (E_{ZDC}) from WA80.¹⁷

6. Mean transverse momentum of direct photons $\langle p_T^{\gamma} \rangle$ as a function of the entropy density derived from the central charged-particle multiplicity plus the participant projectile nucleons calculated from the energy flux in the "projectile fragmentation calorimeter". Data from WA80²²

7. Transverse energy distributions from the NA34 Collaboration²⁴ for 60 and 200 GeV/nucleon ¹⁶O on Al, Ag and W for the range $-0.1 < \eta_{lab} < 2.9$. The curves correspond to fits to a geometrical overlap integral with the smaller impact parameters contributing to successively higher E_{\perp} 's.

8. Energy density distributions for 60 GeV/n (squares) and 200 GeV/n (circles) ¹⁶O + Au calculated from the transverse energy data¹⁷ of WA80 using the Bjorken formula.²⁵

9. Maximum likelihood contours of projections onto the three possible planes of (R_T, R_L, Λ) parameter space. Gaussian fits were performed to the intervals $1 < y < 4$ and $2 < y < 3$ in the Hanbury Brown and Twiss two pion correlation analysis of NA35.²⁷ The solid curve corresponds to a 1σ contour and the dashed curve to 2σ .

PHASE DIAGRAM FOR NUCLEAR MATTER

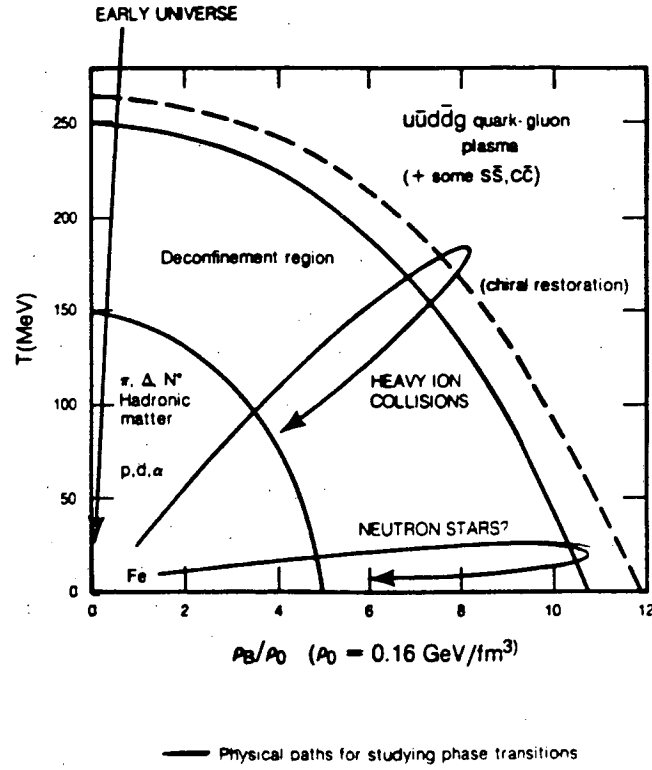
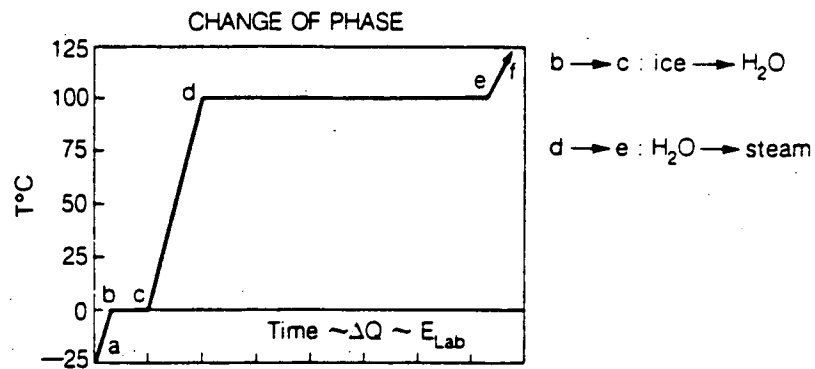


Figure 1 .



The temperature remains constant during each change of phase.

Figure 2 .

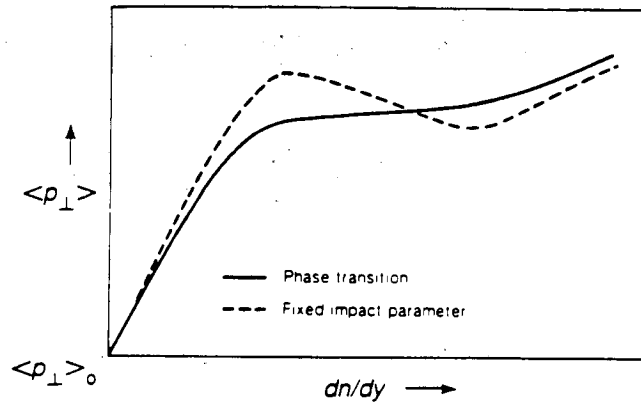
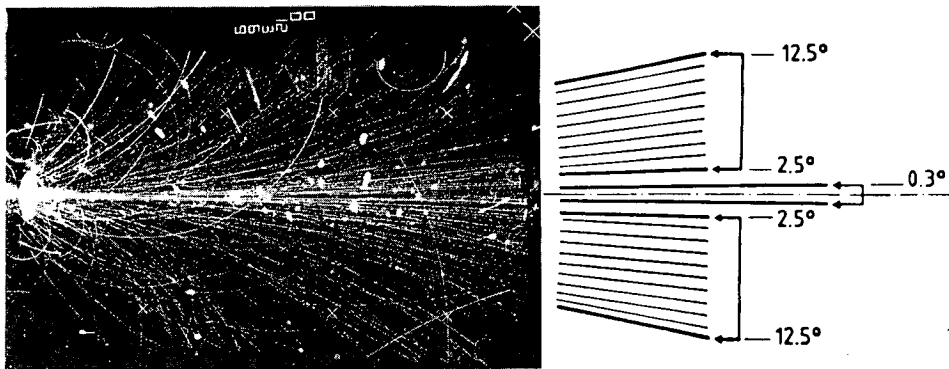


Figure 3 .



XBB 886-6409

Figure 4 .

200 A GeV $^{16}\text{O} + \text{Au}$

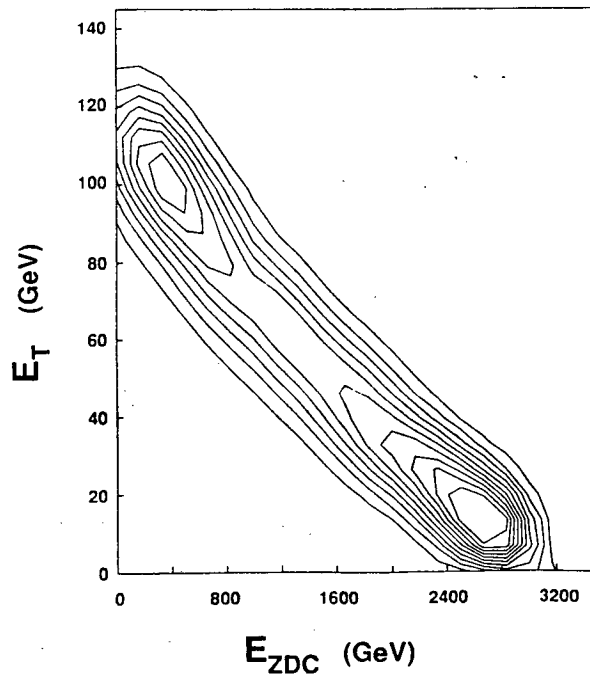


Figure 5 .

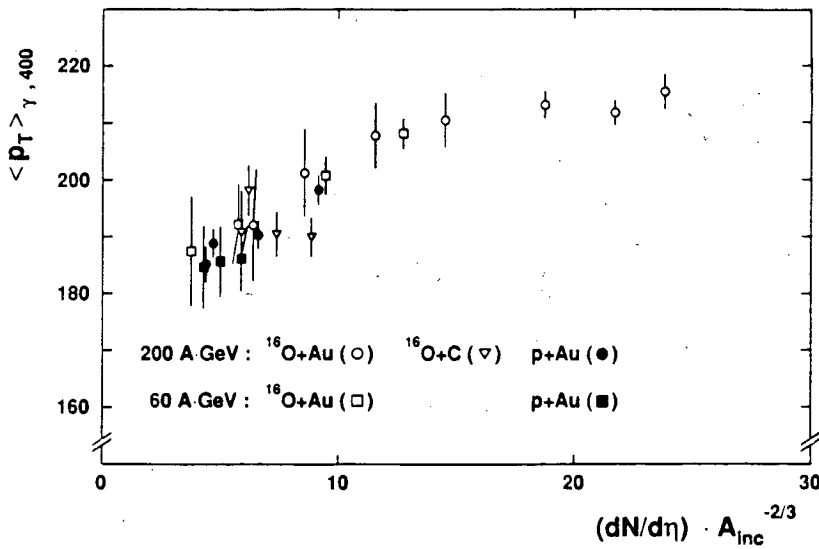


Figure 6 .

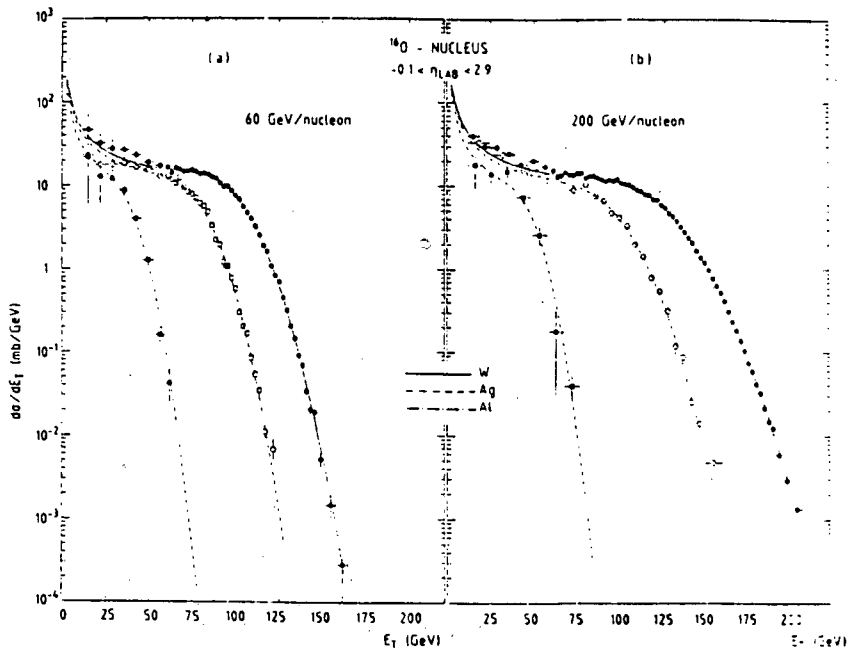


Figure 7 .

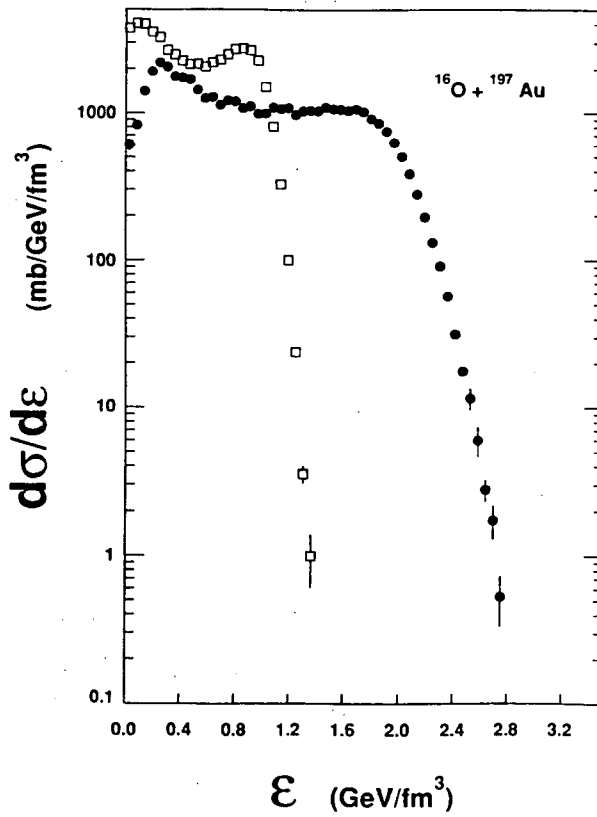


Figure 8 .

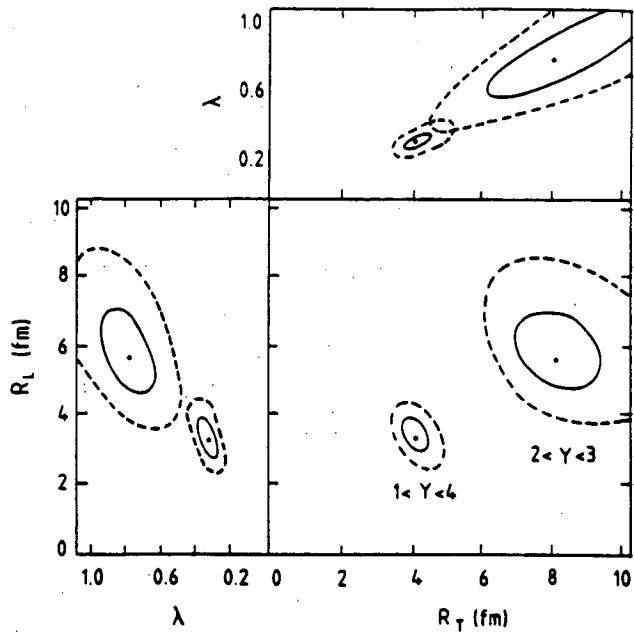


Figure 9 .

LAWRENCE BERKELEY LABORATORY
TECHNICAL INFORMATION DEPARTMENT
UNIVERSITY OF CALIFORNIA
BERKELEY, CALIFORNIA 94720